Iranian Journal of Numerical Analysis and Optimization
Vol. 6, No. 2, (2016), pp 51-64

Controlling semi-convergence phenomenon in non-stationary simultaneous iterative methods

T. Nikazad* and M. Karimpour

Abstract

When applying the non-stationary simultaneous iterative methods for solving an ill-posed set of linear equations, the error usually initially decreases but after some iterations, depending on the amount of noise in the data, and the degree of ill-posedness, it starts to increase. This phenomenon is called semi-convergence. We study the semi-convergence behavior of the non-stationary simultaneous iterative methods and obtain an upper bound for data error (noise error). Based on this bound, we propose new ways to specify the relaxation parameters to control the semi-convergence. The performance of our strategies is shown by examples taken from tomographic imaging.

Keywords: Simultaneous iterative methods; Semi-convergence; Relaxation parameters; Tomographic imaging.

1 Introduction

A mark-point in the history of medical imaging, was the discovery by Wilhelm Röntgen in 1895 of x-rays [10, 22]. The problem of generating medical images from measurements of the radiation around the body of a patient was considered much later. Hounsfield patented the first CT-scanner in 1972 (and was awarded, together with Cormack, in 1979 the Nobel Prize for this invention). This reconstruction problem belongs to the class of inverse problems, which are characterized by the fact that the information of interest is not directly available for measurements. The imaging device (the camera) provides measurements of a transformation of this information. In practice, these measurements are both imperfect (sampling) and inexact (noise).

*Corresponding author
Received 8 April 2015; revised 6 December 2015; accepted 23 Feburary 2016
T. Nikazad
School of Mathematics, Iran University of Science and Technology, Tehran , Iran. e-mail: tnikazad@iust.ac.ir

M. Karimpour
School of Mathematics, Iran University of Science and Technology, Tehran , Iran. e-mail: mkarimpoursb@yahoo.com

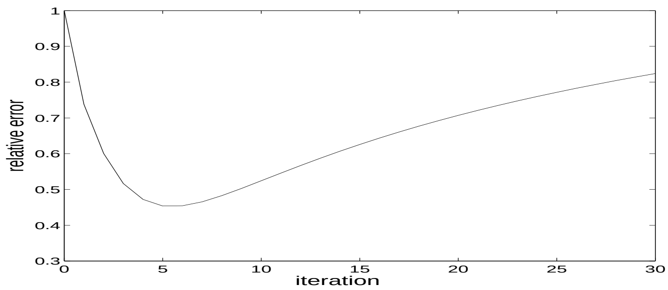

Figure 1: Semi-convergence phenomenon

The mathematical basis for tomographic imaging was laid down by Johann Radon already in 1917 [20]. The word tomography means "reconstruction from slices". It is applied in Computerized (Computed) Tomography (CT) to obtain cross-sectional images of patients. Fundamentally, tomographic imaging deals with reconstructing an image from its projections. The relationship between the unknown distribution (or object) and the physical quantity which can be measured (the projections) is referred to as the forward problem. For several imaging techniques, such as CT, the simplest model for the forward problem involves using the Radon transform R, see [1, 16, 18]. If χ denotes the unknown distribution and β the quantity measured by the imaging device, we have

$$R\chi = \beta.$$

The discrete problem, which is based on expanding χ in a finite series of basis-functions, can be written as

$$Ax \simeq b, \tag{1}$$

where the vector b is a sampled version of β and the vector x, in the case of pixel-(2D) or voxel-(3D) basis, is a finite representation of the unknown object. The matrix $A \in \mathbb{R}^{m\times n}$, typically large and sparse, is a discretization of the Radon transform. An approximative solution to this linear system could be computed by iterative methods, which only require matrix-vector products and hence do not alter the structure of A.

Initially the iteration vectors approach a regularized solution while continuing the iteration often leads to iteration vectors corrupted by noise. This phenomenon is called semi-convergence by Natterer [18]; for analysis of the phenomenon, see, e.g., [1,2,9,11,13,19,21]. The typical overall error behavior is shown in Figure 1.

The Algebraic Reconstruction Technique (ART) is a fully sequential method, and has a long history and rich literature. Originally it was proposed by Kaczmarz [15], and independently, for use in image reconstruction by [13]. The vector of unknowns is up-dated at each equation of the system, after which the next equation is addressed. In the simultaneous algorithms the current iterate is first projected on all sets to obtain intermediate points, and then the next iterate is made by an averaging process, as convex combination, of intermediate points. The prototype of these algorithms is the well-known Cimmino method [5]. We now explain block-iterative method. The basic idea of a block-iterative algorithm is to partition the data A and b of the system (1) into blocks of equations (rows) and treat each block according to the rule used in the simultaneous algorithm for the whole system, passing, e.g., cyclically over all the blocks, see Figure 2.

An iteration vector of the non-stationary simultaneous iterative method (SIM) is defined as follows

$$x_{k+1} = x_k + \lambda_k A^T M(b - Ax_k), \quad k = 0, 1, \cdots \tag{2}$$

with $x_0 \in \mathbb{R}^n$ where $\{\lambda_k\}_{k=1}^{\infty}$ are relaxation parameters and M is a given symmetric positive definite (SPD) matrix which depends on the particular method. In some papers in image reconstruction from projections, the term "simultaneous iterative reconstruction technique (SIRT)" is used for "SIM"; see, e.g., [7, 8, 21]. Several well-known simultaneous methods can be written as (2) for appropriate choices of the matrix M. With $M = I$ we get the classical Landweber method [17]. Choosing $M = \frac{1}{m}\text{diag}(1/\|a_i\|^2)$ where a_i denotes the ith row of A leads to Cimmino's method [5]. The CAV method [4] uses $M = \text{diag}(1/\sum_{j=1}^{n} N_j a_{ij}^2)$ where N_j is the number of non-zeroes in the jth column of A.

We study semi-convergence behavior of the non-stationary SIM, when applied to noisy data. Our main focus is to propose some techniques for updating relaxation parameters to control the data error. Having a reliable stopping rule leads to stop the iterative method in an iteration which makes a proper approximation of the sought solution. Otherwise, we may stop the iteration process early or far from a proper iteration index. For this reason we introduce relaxation parameters to postpone the semi-convergence phenomenon.

The iteration index of an iterative method may be considered as a regularizing parameter. We explain this a bit more. Let x^* be the sought solution using exact data and let $\bar{x}_k$ and x_k denote the iterate using noisy and exact data respectively. Then we have

$$\|\bar{x}_k - x^*\| \leq \|\bar{x}_k - x_k\| + \|x_k - x^*\|. \tag{3}$$

Therefore, the error decomposes into two components, the data error (or noise error) and the approximation error (or iteration error). The semi-convergence of the iteration interplays between these two error terms.

The semi-convergence behavior of the SIM with constant relaxation parameter is analyzed in [8] where the related M-matrix is a symmetric positive definite (SPD) matrix. Based on this stationary, they suggest two strate-

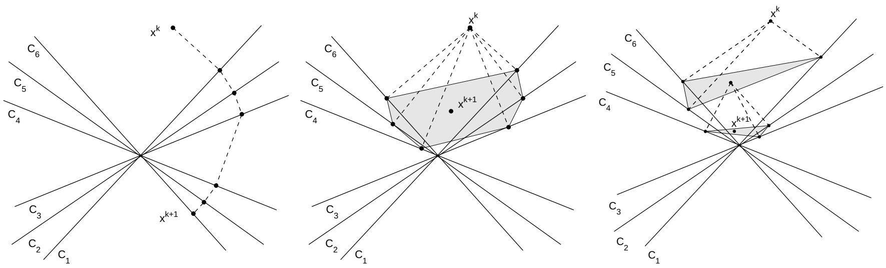

Figure 2: (right to left) sequential method, simultaneous method and sequential block-iterative method

gies for picking relaxation parameters to control the upper bound of data error. The obtained sequence of relaxation parameters is nonnegative and nonascending.

Later in [7], the projected version of the non-stationary SIM is studied where the M-matrix is again assumed SPD. As [8], they consider nonascending sequence of relaxation parameters and emphasize both strategies of [8]. In [7], using nonexpansivity of the projection operator leads to assuming two cases, i.e., the full column-rank problem ($rank(A) = n$) and the rank-deficient problem ($rank(A) < n$) which is handled by a slightly modified problem. Furthermore, they present upper bounds for noise error and iteration error where $rank(A) = n$, see [7, Theorems 3.3 and 3.8] respectively. Also those bounds can be achieved for the modified problem with an unknown regularization parameter (see [7, (3.22),(3.23)]) under some assumptions [7, Lemma 3.9]. In section 2, we give an analysis of non-stationary SIM without having any restriction on $rank(A)$. Additional to strategies given in [8] and [7], we introduce another strategy for choosing relaxation parameters which is able to make more reduction in noise error upper bound comparing with the old strategies.

In Section 3, we consider SIM and give its semi-convergence analysis with three strategies for picking relaxation parameters. We demonstrate the performance of our strategies by examples taken from tomographic imaging in Section 4.

2 Simultaneous iterative algorithm

In this section we give an analysis of the non-stationary SIM without assuming any restriction on $rank(A)$.

Let $\|x\| = \sqrt{x^T x}$ and $\|x\|_M = \sqrt{x^T M x}$ denote the 2-norm and a weighted Euclidean norm respectively. Also, let $M^{1/2}$ and $\rho(Q)$ denote the square root of M and the spectral radius of Q respectively. For $W \in \mathbb{R}^{m\times n}$, we use $N(W)$ and $R(W)$ to denote the null space and range of W respectively. The orthogonal projection from $\mathbb{R}^n$ onto $N(W)$ is denoted by $P(W)$. Also the orthogonal complement of a subspace K of $\mathbb{R}^n$ is denoted by $K^{\perp}$. Here $x_M(A,b)$ denotes a solution of $\min \|Ax-b\|_M$ with the minimal Euclidean norm.

The convergence analysis of SIM can be obtained in, e.g., [14, Theorem II.3] and [3].

Theorem 1. *Let $\rho = \rho(A^TMA)$ and assume that $0 \leq \epsilon \leq \lambda_k \leq (2-\epsilon)/\rho$. If $\epsilon > 0$, or $\epsilon = 0$ and $\Sigma_{k=0}^{\infty} \min(\rho\lambda_k, 2-\rho\lambda_k) = \infty$, then the iterates of (2) converge to $x_M(A,b) + P(A)x_0$.*

2.1 The error in the k-th iteration

As we mentioned before, in this section, we give the same upper bound as [7, Theorems 3.3 and 3.5] but without any restriction on $rank(A)$. Based on our analysis, we give another strategy for choosing relaxation parameters. This strategy is capable to reduce noise error upper bound more than the old strategies given in [8] and [7].

Let $B = A^TMA$, $x^* = x_M(A,b)$ and consider the singular value decomposition (SVD) of $M^{1/2}A$ as

$$M^{1/2}A = U\Sigma V^T$$

where $\Sigma = \text{diag}(\sigma_1, ..., \sigma_p, 0, ..., 0) \in \mathbb{R}^{m\times n}$ with $\sigma_1 \geq \sigma_2 \geq ... \geq \sigma_p > 0$ and p is the rank of A. Let $z_k = x_k - x^*$. Using (2) we have

$$z_{k+1} = z_k + \lambda_k A^T M(b - Az_k - Ax^*) = (I - \lambda_k B)z_k$$

which leads to

$$z_k = \prod_{i=0}^{k-1}(I - \lambda_{k-1-i}B)z_0.$$

Since $z_0 = x_0 - x^*$, we obtain

$$x_k = x^* + \prod_{i=0}^{k-1}(I - \lambda_{k-1-i}B)(x_0 - x^*). \tag{4}$$

Using the orthogonal decomposition theorem, we have $\mathbb{R}^n = N(B) \oplus N(B)^{\perp}$ and $N(B)^{\perp} = R(B)$. Therefore we get $x_0 = \hat{x}_0 + P(B)x_0$ where $\hat{x}_0 \in N(B)^{\perp}$ and $P(B)x_0 \in N(B)$. Thus we can rewrite (4) as

$$x_k = x^* + \prod_{i=0}^{k-1}(I - \lambda_{k-1-i}B)\left(\hat{x}_0 + P(B)x_0 - x^*\right). \tag{5}$$

Since $BP(B)x_0 = 0$ and $P(B) = P(A)$, we obtain

$$\prod_{i=0}^{k-1}(I - \lambda_{k-1-i}B)P(B)x_0 = P(B)x_0 = P(A)x_0. \tag{6}$$

Since $\hat{x}_0,\ x^* \in N(B)^\perp$, we can rewrite $\hat{x}_0 - x^*$ as

$$\hat{x}_0 - x^* = \sum_{j=1}^{p} c_j v_j \tag{7}$$

where c_j and v_j are scalar and the j-th column of V respectively. Using (5), (6), (7) and the SVD of B, we obtain the following expression for the k-th iteration

$$\begin{aligned} x_k &= x^* + P(A)x_0 + \prod_{i=0}^{k-1}(I - \lambda_{k-1-i}V\Sigma^T\Sigma V^T)(\sum_{j=1}^{p} c_j v_j) = x^* + P(A)x_0 + \\ &+ V\mathrm{diag}\left(\prod_{i=0}^{k-1}(1-\lambda_i\sigma_1^2), \ldots, \prod_{i=0}^{k-1}(1-\lambda_i\sigma_p^2), 1, \ldots, 1\right) V^T \sum_{j=1}^{p} c_j v_j \\ &= x^* + P(A)x_0 + \sum_{j=1}^{p}\prod_{i=0}^{k-1}(1-\lambda_i\sigma_j^2)c_j v_j. \end{aligned} \tag{8}$$

Let $\overline{b} = b + \delta b$ and

$$\overline{x}_{k+1} = \overline{x}_k + \lambda_k A^T M(\overline{b} - A\overline{x}_k) \tag{9}$$

where δb is the perturbation consisting of additive noise. Setting $\overline{z}_k = \overline{x}_k - x^*$, we get

$$\begin{aligned} \overline{z}_k &= \overline{z}_{k-1} + \lambda_{k-1}A^T M(b + \delta b - A\overline{z}_{k-1} - Ax^*) \\ &= (I - \lambda_{k-1}B)\overline{z}_{k-1} + \lambda_{k-1}A^T M\delta b \\ &= \prod_{i=0}^{k-1}(I - \lambda_{k-1-i}B)z_0 + \sum_{i=0}^{k-2}\prod_{j=i+1}^{k-1}(I - \lambda_{k-1-j}B)\lambda_i A^T M\delta b + \\ &+ \lambda_{k-1}A^T M\delta b. \end{aligned} \tag{10}$$

Since $\overline{x}_0 = x_0$, similar to (8), we have

$$\overline{x}_k = x^* + P(A)x_0 + \sum_{j=1}^{p} \prod_{i=0}^{k-1} (1-\lambda_i \sigma_j^2) c_j v_j +$$
$$+ \sum_{i=0}^{k-2} \prod_{j=i+1}^{k-1} (I - \lambda_{k-1-j} B) \lambda_i A^T M \delta b + \lambda_{k-1} A^T M \delta b. \tag{11}$$

We now assume that the sequence of relaxation parameters is nonnegative and nonascending, i.e.,

$$0 < \lambda_{i+1} \le \lambda_i \tag{12}$$

and consider the following function introduced in [8]

$$\Psi^k(\sigma, \lambda) = \frac{1-(1-\lambda\sigma^2)^k}{\sigma}. \tag{13}$$

Theorem 2. *Let* $\omega = \|M^{1/2}\delta b\|$ *and* $0 < \lambda_k \le \frac{1}{\sigma_1^2}$. *The noise error of SIM is bounded above by*

$$\|\overline{x}_k - x_k\| \le \frac{\omega \lambda_0 \sigma_1}{\lambda_{k-1}\sigma_p} \Psi^k(\sigma_p, \lambda_{k-1}). \tag{14}$$

Proof. By subtracting (8) and (11), we obtain

$$\overline{x}_k - x_k = \sum_{i=0}^{k-2} \prod_{j=i+1}^{k-1} (I - \lambda_{k-1-j} B) \lambda_i A^T M \delta b + \lambda_{k-1} A^T M \delta b. \tag{15}$$

Therefore we have

$$\|\overline{x}_k - x_k\| \le \sum_{i=0}^{k-2} \lambda_i \left\| \prod_{j=i+1}^{k-1} (I - \lambda_{k-1-j} B) A^T M \delta b \right\| + \lambda_{k-1} \|A^T M \delta b\|. \tag{16}$$

Using the SVD of $M^{1/2}A$, we get that

$$\prod_{j=i+1}^{k-1} (I - \lambda_{k-1-j} B) A^T M^{1/2} = V \prod_{j=i+1}^{k-1} (I - \lambda_{k-1-j} \Sigma^T \Sigma) V^T V \Sigma^T U^T$$
$$= V W_{i,k} U^T$$

where

$$W_{i,k} = \operatorname{diag}\left(\prod_{j=i+1}^{k-1} (1-\lambda_j \sigma_1^2)\sigma_1, \ldots, \prod_{j=i+1}^{k-1} (1-\lambda_j \sigma_p^2)\sigma_p, 0, \ldots, 0 \right).$$

Using (12) and $0 < \lambda_k \le \frac{1}{\sigma_1^2}$, we obtain

$$\left\| \prod_{j=i+1}^{k-1} (I - \lambda_{k-1-j} B) A^T M^{1/2} \right\| \le \|W_{i,k}\| = \max_{1\le s\le p} \left\| \prod_{j=i+1}^{k-1} (1 - \lambda_j \sigma_s^2)\sigma_s \right\|$$
$$\le \sigma_1 (1 - \lambda_{k-1}\sigma_p^2)^{k-1-i}. \quad (17)$$

Since $\|A^T M \delta b\| \le \sigma_1 \omega$, we conclude that, using (12),(17) and the assumptions of theorem,

$$\begin{aligned} \|\overline{x}_k - x_k\| &\le \sum_{i=0}^{k-2} \lambda_0 \omega \left\| \prod_{j=i+1}^{k-1} (I - \lambda_{k-1-j} B) A^T M^{1/2} \right\| + \lambda_0 \sigma_1 \omega \\ &\le \sum_{i=0}^{k-2} \lambda_0 \omega \sigma_1 (1 - \lambda_{k-1}\sigma_p^2)^{k-1-i} + \lambda_0 \sigma_1 \omega \\ &= \sum_{s=0}^{k-1} \lambda_0 \omega \sigma_1 (1 - \lambda_{k-1}\sigma_p^2)^{s} \\ &= \frac{\omega \lambda_0 \sigma_1}{\lambda_{k-1}\sigma_p} \frac{1 - (1 - \lambda_{k-1}\sigma_p^2)^k}{\sigma_p} \\ &= \frac{\omega \lambda_0 \sigma_1}{\lambda_{k-1}\sigma_p} \Psi^k(\sigma_p, \lambda_{k-1}). \end{aligned}$$

This completes the proof. □

Remark 1. To obtain a similar result as (14) where the projected case of (2) is employed, we refer to [7, Theorem 3.3] where it is assumed $rank(A) = n$.

Similar to [8], we consider the equation

$$g_{k-1}(y) = (2k-1)y^{k-1} - (y^{k-2} + \cdots + y + 1) = 0 \quad (18)$$

which has a unique real root $\zeta_k \in (0,1)$. The roots satisfy $0 < \zeta_k < \zeta_{k+1} < 1$ and $\lim_{k\to\infty} \zeta_k = 1$ (see [8, Propositions 2.3, 2.4]), and they can easily be precalculated, see Table 1.

Again, let σ_1 denote the largest singular value of $M^{1/2}A$. Then we have the following alternative upper bound for the noise error.

Theorem 3. *Assume that* $\sigma_1 \le 1/\sqrt{\lambda_{k-1}}$*; then*

$$\|x_k - \bar{x}_k\| \le \frac{\omega \lambda_0 \sigma_1}{\sqrt{\lambda_{k-1}}\sigma_n} \frac{1 - \zeta_k^k}{\sqrt{1 - \zeta_k}}, \quad (19)$$

where ζ_k *is the unique root in* $(0,1)$ *of* (18).

Table 1: The unique root $\zeta_k \in (0,1)$ of $g_{k-1}(y) = 0$, cf. (18), as function of the iteration index k

k	ζ_k	k	ζ_k	k	ζ_k	k	ζ_k	k	ζ_k	k	ζ_k
2	0.3333	7	0.8156	12	0.8936	17	0.9252	22	0.9424	27	0.9531
3	0.5583	8	0.8392	13	0.9019	18	0.9294	23	0.9449	28	0.9548
4	0.6719	9	0.8574	14	0.9090	19	0.9332	24	0.9472	29	0.9564
5	0.7394	10	0.8719	15	0.9151	20	0.9366	25	0.9493	30	0.9578
6	0.7840	11	0.8837	16	0.9205	21	0.9396	26	0.9513	31	0.9592

Proof. Using [8, Proposition 2.3] we obtain the following bound for the function $\Psi^k(\sigma, \lambda)$ appearing in (14):

$$\max_{1\le i\le n} \Psi^k(\sigma_i, \lambda_{k-1}) \le \max_{0<\sigma\le\sigma_1} \Psi^k(\sigma, \lambda_{k-1}) \le \max_{0<\sigma\le 1/\sqrt{\lambda_{k-1}}} \Psi^k(\sigma, \lambda_{k-1}) \le \sqrt{\lambda_{k-1}}\frac{1-\zeta_k^k}{\sqrt{1-\zeta_k}}. \quad (20)$$

The assumption in the theorem implies

$$\sigma_1 \le 1/\sqrt{\lambda_{k-1}} \quad \Leftrightarrow \quad \lambda_{k-1} \le 1/\sigma_1^2. \quad (21)$$

Then by (14) and (20), and assuming (21), we obtain the bound in (19). □

Remark 2. The case $\lambda_{k-1} \in (1/\sigma_1^2, 2/\sigma_1^2)$ is discussed in [8, Remark 2.2].

3 Choice of relaxation parameters

Using (19), we propose following strategies for choosing relaxation parameters:

$$\Psi_1 - rule: \quad \lambda_k = \begin{cases} \frac{\sqrt{2}}{\sigma_1^2}, & \text{for } k = 0,1 \\ \frac{2}{\sigma_1^2}(1-\zeta_k), & \text{for } k \ge 2, \end{cases} \quad (22)$$

$$\Psi_2 - rule: \quad \lambda_k = \begin{cases} \frac{\sqrt{2}}{\sigma_1^2}, & \text{for } k = 0,1 \\ \frac{2}{\sigma_1^2}(1-\zeta_k)(1-\zeta_k^k)^{-2}, & \text{for } k \ge 2 \end{cases} \quad (23)$$

$$\Psi_3 - rule: \quad \lambda_k = \begin{cases} \frac{\sqrt{2}}{\sigma_1^2}, & \text{for } k = 0,1 \\ \frac{2}{\sigma_1^2}(1-\zeta_k)^{r-1}(1-\zeta_k^k)^{2}, & \text{for } k \ge 2 \end{cases} \quad (24)$$

where $\{\zeta_k\}_{k\ge2}$ are the roots of (18) and $1 < r \le 2$.

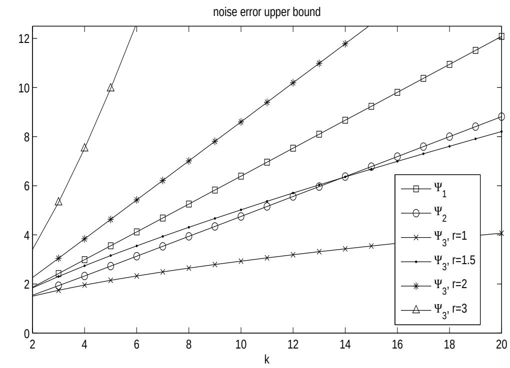

Figure 3: Noise error upper bound (25) for different strategies with the factor ω/σ_p omitted

Remark 3. Using (19) and strategies (22-24), we have the following upper bounds for noise error

$$\|\overline{x}_k - x_k\| \leq \begin{cases} \frac{\omega}{\sigma_p}(1-\zeta_k^k)(1-\zeta_k)^{-1}, & \Psi_1 \\ \frac{\omega}{\sigma_p}(1-\zeta_k^k)^2(1-\zeta_k)^{-1}, & \Psi_2 \\ \frac{\omega}{\sigma_p}(1-\zeta_k)^{-r/2}, & \Psi_3 \end{cases} \tag{25}$$

for $k \geq 2$.

Figure 3 shows the behavior of noise error upper bound (25) for different strategies. As it seen, Ψ_3 with $r = 1$ and Ψ_3 with $r = 3$ give the smallest and largest upper bounds respectively. Furthermore, Ψ_3 with $r = 1.5$ gives smaller upper bound than Ψ_1 and Ψ_2.

Remark 4. It is easy to check that, using [8, Theorems 3.1 and 3.3], the both strategies (22) and (23) satisfy all conditions of Theorem 1. Therefore, the sequence x_k generated by (2) converges to $x_M(A,b) + P(A)x_0$.

Next we will check that the relaxation parameters defined in (24) satisfy all conditions of Theorem 1.

Proposition 1 *The sequence generated by (2) with strategies (24) converges to $x_M(A,b)$.*

Proof. Since $\rho = \sigma_1^2$, we have $0 \leq \rho\lambda_k \leq 2$. Using [8, (2.17), (3.10)], we obtain that

$$\begin{aligned}\sum_{k\geq 2}(1-\zeta_k)^{r-1}(1-\zeta_k^k)^2 &> \sum_{k\geq 2}\left(1-\frac{2k}{2k+1}\right)^{r-1}\left(1-\frac{k-1}{2k-1}\right)^2\\ &= \sum_{k\geq 2}\left(\frac{1}{2k+1}\right)^{r-1}\left(\frac{k}{2k-1}\right)^2\\ &> \sum_{k\geq 2}\frac{k^2}{(2k+1)^{r+1}}. \end{aligned} \tag{26}$$

It is clear that (26) diverges if $r \leq 2$. Therefore, we have $\Sigma_{k\geq 2}\lambda_k = \infty$. It is easy to check that $\min\{\rho\lambda_k, 2-\rho\lambda_k\} = \rho\lambda_k$ for k sufficiently large. Thus, all conditions of Theorem 1 hold and consequently the sequence x_k generated by (2) converges to $x_M(A,b) + P(A)x_0$. □

4 Numerical results

In this section we give two examples of computerized tomography field. We used 5% and 10% white Gaussian noises to produce noisy data. The constant optimal relaxation parameter λ_{opt} refers to the strategy when a constant value of the relaxation parameter is used, chosen such that it gives rise to the smallest relative error within 20 iterations. For the choices of M matrix in SIM, we always use Cimmino's method. We compare our results with cgne which is a Krylov-type method. The method cgne is sometimes also called cgls. This method is scaled by $M^{1/2}$, i.e., using $M^{1/2}A$, $M^{1/2}b$ instead of A, b.

As we mentioned before, Theorems 2 and 3 and the strategies (22-24) are based on (12). Note that the convergence analysis is not based on the nonascending property. Since $\zeta_k < \zeta_{k+1}$ and using [8, Proposition 3.3], both strategies (22) and (23) satisfy (12). For the the third strategy (24) we have

$$\begin{aligned}(1-\zeta_k)^{r-1}(1-\zeta_k^k)^2 &> (1-\zeta_{k+1})^{r-1}(1-\zeta_k^k)^2\\ &> (1-\zeta_{k+1})^{r-1}(1-\zeta_{k+1}^{k+1})^2\end{aligned}$$

provided that

$$\zeta_{k+1}^{k+1} > \zeta_k^k. \tag{27}$$

We do not have any mathematical proof which shows (27) holds but our numerical tests verifies (27) where $r \geq 1$.

Our first tests are based on the standard head phantom from [13]. We report some numerical tests with an example taken from the field of tomographic image reconstruction from projections, using the SNARK09 software package [6]. The phantom is discretized into 63×63 pixels, and 16 projections (evenly distributed between 0 and 174 degrees) with 99 rays per projection

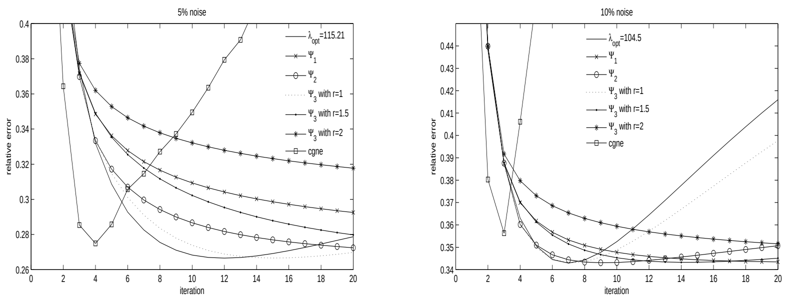

Figure 4: Relative error histories in SIM using small phantom with different relaxation strategies

are used. The resulting matrix A has dimension 1584×3969, so that the system of equations is highly underdetermined. Figure 4 shows the error histories for SIM, using the optimal fixed relaxation parameter as well as Ψ_1, Ψ_2 and Ψ_3 strategies with noisy data.

Based on behavior of noise error upper bound, see Figure 3, using Ψ_3 with $r = 1$ gives the smallest upper bound. This fact is confirmed by Figure 4 (left) where 5% noise is used. But using 10% noise, Figure 4 (right), leads to fast semi-convergence. The reason could be the large value of ω in (19) which is eliminated in all strategies. However, the results of Ψ_3 rule with $r = 1.5$ and Ψ_1 rule are proper where 10% noise is used.

In our second example we used the (matlab-based) package AIRtools [12] to produce the phantom, the matrix and the right-hand side (with and without noise). We again used 5% and 10% white Gaussian noises. The phantom is now discretized into 365×365 pixels. We take 88 projections (evenly distributed between 0 and 179 degrees) with 516 rays per projection. The resulting projection matrix A has dimension 40892×133225, so that again the system of equations is underdetermined. Figure 4 shows the relative error histories of SIM with noisy data. As it is seen, this figure shows that the results of Ψ_3 rule with $r = 1$ are close to the results of optimal rule.

For both noise levels and phantoms, cgne is the fastest method. However it also shows a distinctive semi-convergence behavior making it more dependent on a reliable stopping rule than SIM with our strategies.

Acknowledgments

We thank Tommy Elfving and Per Christian Hansen for their valuable comments. We wish to thank two anonymous referees for constructive criticism and helpful suggestions which improved our paper.

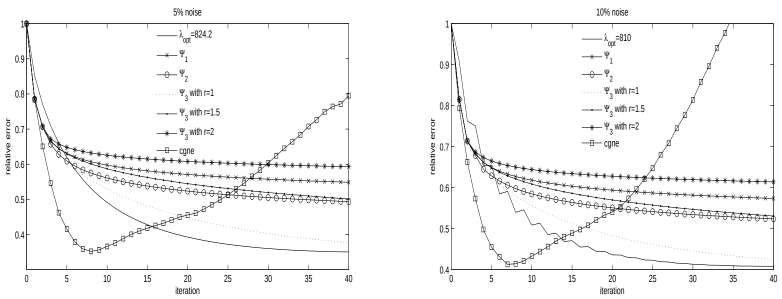

Figure 5: Relative error histories in SIM using the big phantom

References

1. Bertero, M. and Boccacci, P. *Introduction to inverse problems in imaging.* CRC press, 1998.

2. Brianzi, P., Benedetto, F.D. and Estatico, C. *Improvement of space-invariant image deblurring by preconditioned landweber iterations.* SIAM Journal on Scientific Computing, 30(3):1430–1458, 2008.

3. Censor, Y. and Elfving, T. *Block-iterative algorithms with diagonally scaled oblique projections for the linear feasibility problem.* SIAM Journal on Matrix Analysis and Applications, 24(1):40–58, 2002.

4. Censor, Y., Gordon, D. and Gordon, R. *Component averaging: An efficient iterative parallel algorithm for large and sparse unstructured problems.* Parallel computing, 27(6):777–808, 2001.

5. Cimmino, G. and Ricerche, C.N.D. *Calcolo approssimato per le soluzioni dei sistemi di equazioni lineari.* Istituto per le applicazioni del calcolo, 1938.

6. R. Davidi, G. T. Herman, and J. Klukowska. Snark09: A programming system for the reconstruction of 2d images from 1d projections. The CUNY Institute for Software Design and Development, New York, 2009.

7. Tommy Elfving, Per Christian Hansen, and Touraj Nikazad. Semiconvergence and relaxation parameters for projected SIRT algorithms. SIAM Journal on Scientific Computing, 34(4):A2000–A2017, 2012.

8. Elfving, T., Nikazad, T. and Hansen, P.C. *Semiconvergence and relaxation parameters for a class of SIRT algorithms,* Electronic Transactions on Numerical Analysis, 37:321–336, 2010.

9. Engl, H.W., Hanke, M. and Neubauer, A. *Regularization of inverse problems*, volume 375. Springer Science & Business Media, 1996.

10. Guy C. and Ffytche, D. *An introduction to the principles of medical imaging,* World Scientific, 2005.

11. Hansen, P.C. *Rank-deficient and discrete ill-posed problems: numerical aspects of linear inversion*, volume 4. Siam, 1998.

12. Hansen, P.C. and Hansen, M.S.*AIR tools-a MATLAB package of algebraic iterative reconstruction methods*, Journal of Computational and Applied Mathematics, 236(8):2167–2178, 2012.

13. Herman, G.T. *Fundamentals of computerized tomography: image reconstruction from projections*, Springer Science & Business Media, 2009.

14. Jiang, M. and Wang, G. *Convergence studies on iterative algorithms for image reconstruction*, Medical Imaging, IEEE Transactions on, 22(5):569–579, 2003.

15. Kaczmarz, S. *Angenherte auflsung von systemen linearer gleichungen.* Bulletin International de lAcademie Polonaise des Sciences et des Lettres, 35:355–357, 1937.

16. Kak, A.C. and Slaney, M. *Principles of computerized tomographic imaging*, volume 33. Siam, 1988.

17. Landweber, L. *An iteration formula for Fredholm integral equations of the first kind,* American journal of mathematics, pages 615–624, 1951.

18. Natterer, F. *The mathematics of computerized tomography,* John Wiley, New York, 1986.

19. Piana, M. and Bertero, M. *Projected landweber method and preconditioning,* Inverse Problems, 13(2):441, 1997.

20. Radon, J. *ber die bestimmung von funktionen durch ihre integralwerte lngs gewisser mannigfaltigkeiten,* Classic papers in modern diagnostic radiology, 5, 2005.

21. Sluis, A. and Vorst, H. *Sirt-and cg-type methods for the iterative solution of sparse linear least-squares problems,* Linear Algebra and its Applications, 130:257–303, 1990.

22. Webb, S. *From the watching of shadows: the origins of radiological tomography,* CRC Press, 1990.

کنترل پدیده شبه همگرایی در روش های تکراری همزمان غیر ایستا

تورج نیک آزاد و مهدی کریم پور

دانشگاه علم و صنعت ایران، دانشکده ریاضی

دریافت مقاله ۲۸ فروردین ۱۳۹۴، دریافت مقاله اصلاح شده ۱۶ آذر ۱۳۹۴، پذیرش مقاله ۵ اسفند ۱۳۹۴

چکیده : هنگام به کارگیری روش های تکراری همزمان غیرایستا برای حل یک دستگاه بدوضع از معادلات خطی، در ابتدا معمولا خطا کاهش می یابد اما پس از چند تکرار بسته به مقدار اختلال موجود در داده ها و میزان بدوضعی دستگاه، خطا شروع به افزایش می کند. این پدیده شبه همگرایی نامیده می شود. ما رفتار شبه همگرایی رابرای روش های تکراری همزمان غیر ایستا بررسی کرده و یک کران بالا برای خطای داده (خطای اختلال) بدست می آوریم. براساس این کران ما راه های جدیدی برای تعیین پارامترهای آزاد به منظور کنترل شبه همگرایی پیشنهاد می کنیم. کارآمدی راهکارهای ما به وسیله مثال هایی که از تصویر پرتونگاری پزشکی آمده اند مشخص می شوند.

کلمات کلیدی : روش های تکراری همزمان؛ شبه همگرایی؛ پارامترهای آزاد؛ تصویر پرتونگاری پزشکی.